Opto-locomotor reflexes of mice to reverse-phi stimuli

Laurens A. M. H. Kirkels Department of Biophysics, Donders Institute, Radboud University, Nijmegen, The Netherlands

Wenjun Zhang Department of Biophysics, Donders Institute, Radboud University, Nijmegen, The Netherlands

Jacob Duijnhouwer Center for Molecular and Behavioral Neuroscience, Rutgers University, Newark, USA

Richard J. A. van Wezel Department of Biophysics, Donders Institute, Radboud University, Nijmegen, The Netherlands
Biomedical Signals and Systems, TechMed Centre, Twente University, Enschede, The Netherlands

In a reverse-phi stimulus, the contrast luminance of moving dots is reversed each displacement step. Under those conditions, the direction of the moving dots is perceived in the direction opposite of the displacement direction of the dots. In this study, we investigate if mice respond oppositely to phi and reverse-phi stimuli. Mice ran head-fixed on a Styrofoam ball floating on pressurized air at the center of a large dome. We projected random dot patterns that were displaced rightward or leftward, using either a phi or a reverse-phi stimulus. For phi stimuli, changes in direction caused the mice to reflexively compensate and adjust their running direction in the direction of the displaced pattern. We show that for reverse-phi stimuli mice compensate in the direction opposite to the displacement direction of the dots, in accordance with the perceived direction of displacement in humans for reverse-phi stimuli.

Introduction

When the contrast of an apparent motion stimulus (phi stimulus) is flipped periodically, the perceived direction of displacement reverses. This perceptual illusion is referred to as a reverse-phi percept (Anstis, 1970; Anstis & Mather, 1985; Anstis & Rogers, 1975). Reverse-phi stimuli have been used to investigate neural mechanisms of visual processing in a wide variety of animals such as monkeys, cats, wallabies, beetles, fruit flies, and zebrafish (Clark, Bursztyn, Horowitz, Schnitzer, & Clandinin, 2011; Emerson, Citron, Vaughn, & Klein, 1987; Hassenstein & Reichardt, 1956; Ibbotson & Clifford, 2001; Krekelberg & Albright, 2005; Livingstone & Conway, 2003; Orger, Smear, Anstis, & Baier, 2000; Tuthill, Chiappe, & Reiser, 2011).

The why and how of reverse-phi motion have been the topics of much debate. Crucial to any explanation of the phenomenon is the detection of motion and correlations across different contrasts. Classical approaches attribute the effect to contrast reversals that shift Fourier energy to the opposite direction, which is picked up by a motion detector tuned to that opposite direction (Adelson & Bergen, 1985; Krekelberg & Albright, 2005; van Santen & Sperling, 1985). Other explanations are based on spatiotemporal correlations between positive and negative contrasts carried by the ON and OFF channels of the visual system, which diverge as early as the level of retinal bipolar cells (Bours, Kroes, & Lankheet, 2009; Duijnhouwer & Krekelberg, 2016; Mo & Koch, 2003; Schiller, 1992; Westheimer, 2007). Recent fly studies using contemporary techniques demonstrate there is still no consensus about the mechanisms underlying the phenomenon (Leonhardt, Meier, Serbe, Eichner, & Borst, 2017; Salazar-Gatzimas, Agrochao, Fitzgerald, & Clark, 2018).

Studies by Mo and Koch (2003) and Bours, Kroes, & Lankheet (2007) proposed models for motion detection that combine inputs from both ON and OFF cells to generate direction selectivity; however, the models offer opposing explanations of the apparent reversal seen in reverse-phi stimuli. The motion detectors proposed by Mo and Koch (2003) are excited by phi stimuli in one direction as well as by reverse-phi stimuli in the opposite direction. The Bours–Lankheet model, however, proposes excitation of motion detectors by phi stimuli and inhibition by reverse-phi stimuli in the

Citation: Kirkels, L. A. M. H., Zhang, W., Duijnhouwer, J., & van Wezel, R. J. A. (2020). Opto-locomotor reflexes of mice to reverse-phi stimuli. *Journal of Vision*, *20*(2):7, 1–10, https://doi.org/10.1167/jov.20.2.7.

https://doi.org/10.1167/jov.20.2.7 Received February 12, 2019; published February 25, 2020 ISSN 1534-7362

same direction. This prediction was investigated by Duijnhouwer and Krekelberg (2016), who measured directional tuning curves of neurons in primary visual and middle temporal cortex areas of awake behaving macaques and claimed some evidence to support the Bours–Lankheet "counterevidence" model.

Although mice have much poorer visual acuity than primates, their visual systems bear relevant similarities. Both animals perceive motion stimuli (Huberman & Niell, 2011; Niell & Stryker, 2008; Priebe & McGee, 2014; Wang, Gao, & Burkhalter, 2011), and they both have separate ON and OFF channels that appear to share evolutionary preserved pathways (Calkins, Tsukamoto, Sterling, & Euler, 1998; Ekesten & Gouras, 2005; Ghosh, Bujan, Haverkamp, Feigenspan, & Wässle, 2004; Grubb & Thompson, 2004; Huberman, Wei, Elstrott, Stafford, Feller, & Barres, 2009; Mataruga, Kremmer, & Müller, 2007; Puller & Haverkamp, 2011; Volland, Esteve-Rudd, Hoo, Yee, & Williams, 2015). Furthermore, a wide variety of techniques are applicable to mice that allow for relating neuronal function in retina and visual cortex to visually driven behavior, such as genetically encoded calcium current and voltage indicators (Akemann, Mutoh, Perron, Rossier, & Knöpfel, 2010; Antic, Empson, & Knöpfel, 2016; Chen et al., 2013; Knöpfel, 2012; Miyawaki et al., 1997; Tian et al., 2009), designer receptors activated by designer drugs (Sternson & Roth, 2014; Wulff & Arenkiel, 2012), and optogenetics (Fenno, Yizhar, & Deisseroth, 2011; Han et al., 2009; Packer, Roska, & Häusser, 2013; Zhang et al., 2007).

Taken together, this could make the mouse an excellent animal model to further study how the ON and OFF pathways interact to give rise to the reverse-phi phenomenon. As a first step, we developed a behavioral experiment to investigate responses of mice to phi and reverse-phi stimuli. We positioned mice head-fixed on a spherical, two-dimensional treadmill and projected randomly positioned black and white dots on a spherical screen surrounding the animal (Harvey, Collman, Dombeck, & Tank, 2009; Hölscher, Schnee, Dahmen, Setia, & Mallot, 2005; Kirkels, Zhang, Havenith, Tiesing, Glennon, Wezel, & Duijnhouwer, 2018; Schmidt-Hieber & Häusser, 2013). We measured the opto-locomotor reflex (OLR) (Kirkels et al., 2018) in response to phi and reverse-phi stimuli to the left and right by recording the rotation of the treadmill along the vertical axis.

Methods

Animals

We used nine male C57BL/6J mice in this experiment. C57BL/6J mice are often used in behavioral studies of mouse vision because their visual acuity and performance are among the best of commonly used strains (Prusky & Douglas, 2003; Wong & Brown, 2006). The starting weights of all animals were then determined (23.2 ± 2.6 g). To maintain a weight between 85% and 95% of their starting weight, the animals received 2.2 g of food per day. Food was increased or decreased if animals fell outside the thresholds. All mice were kept in a well-ventilated, temperature-controlled room (21 ± 2°C) with a 12/12-hour light/dark cycle. All experiments were conducted in compliance with Dutch and European laws and regulations and were approved by the animal ethical committee of Radboud University Nijmegen. All experiments adhered to the Association for Research in Vision and Ophthalmology Statement for the Use of Animals in Ophthalmic and Vision Research.

Surgery

Anesthesia was induced and maintained via a nose cone during surgery (4% isoflurane in oxygen at induction, 1.0%–1.5% during surgery). After the animals were anesthetized, they were placed in a stereotact and their eyes covered in sterile ocular lube (Puralube; Dechra, Northwich, UK) to prevent eye dehydration. Next, the head of the animal was shaved and the skin on top of the head was removed using fine scissors. A local anesthetic compound (1 mg/ml lidocaine hydrochloride with 0.25 mg/ml bupivacaine) was applied to the exposed periosteum, and the skull was cleaned thoroughly with a bone scraper. Dental cement (SuperBond C&B; Sun Medical, Rising Sun, IN) was used to fix a custom-made titanium head plate to the skull. This head plate allowed fixation of the head during the experiments.

Habituation

The mice were handled and head-fixed in the set-up for 10 minutes after 1 week of recovery from the surgery. The duration of this exposure to the set-up increased gradually over the following 5 days to two sessions of 40 minutes each per day. Animals were running spontaneously during large parts of a session, requiring no reward; therefore, no specific training beyond general habituation to the set-up was required.

Visual stimulation

Stimuli consisted of white dots (0.78 cd/m^2) and black dots (0.24 cd/m^2) with a radius of 1.4° on a mid-gray background (0.51 cd/m^2). We used an Optoma X501 (New Taipei City, Taiwan) video projector

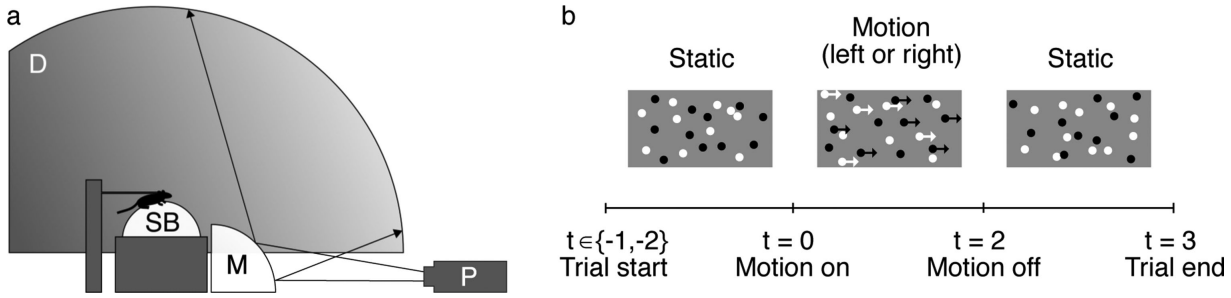

Figure 1. (a) Schematic drawing of the set-up. A projector (P) displayed patterns of randomly positioned dots via a mirror (M) onto the inside of a dome (D). Mice ran under head-fixed conditions on a Styrofoam ball (SB) floating on air. (b) Schematic of the stimulus and timing (see Visual stimulation section for details).

(resolution: 1920 × 1080 at 60 Hz) to project the stimuli, via a quarter-spherical mirror, onto the inside of a dome made of fiberglass-reinforced resin (Fibresports UK, Basildon, UK) with an inner diameter of 112 cm (Figure 1a). We placed the mouse on a treadmill consisting of a Styrofoam ball floating on air in a custom-made socket (University College London workshops) at the center of this dome. The display area covered 220° of visual angle horizontally and from 10° below the mouse to 80° above it vertically (for details, see Kirkels et al., 2018).

The motion stimuli were based on the single-step dot lifetime (SSDL) paradigm (Morgan & Ward, 1980), with randomly positioned dots making a single horizontal displacement and then being randomly repositioned in the display area. Each frame contained 1000 dots, half of which were newly created and half of which were displaced dots. For phi stimuli, the dots maintained their luminance polarity (white or black) during displacement, whereas in reverse-phi stimuli the polarity of the dots reversed. The use of SSDL is crucial for clean reverse-phi stimulation. If the dots were instead to move for multiple steps while flipping their contrast polarity, every two-back step would be a regular phi-motion correlation. Similar stimuli have been used before (Bours, Kroes, & Lankheet, 2007, 2009; Bours, Stuur, & Lankheet, 2007; Duijnhouwer & Krekelberg, 2016).

Trials started with the displacement parameter set to zero, resulting in a flickering display with no net direction. After either 1 or 2 seconds, the dots started moving with single steps to the left or right for 2 seconds, followed by another stationary flickering period of 1 second (Figure 1b). The 1- or 2-second durations of the initial static phase were randomly interleaved to reduce the animal's ability to anticipate motion onset.

We created displacements by incrementing (or decrementing) the azimuths of the dots at each 17-ms video frame, resulting in a rotation around the vertical axis, or yaw. We varied the temporal interval from 1 to 7 times the frame duration of the video frame (17–117 ms) while adjusting the displacement size (0.6°–4.2°) to maintain a speed of always 36°/s. The resulting 56 conditions (seven temporal intervals, two onset delays, phi/reverse-phi, left/right) were randomly interleaved and repeated three times per session. Each mouse completed at least 32 sessions.

Recording and data analysis

The two-dimensional treadmill consisted of a Styrofoam ball (diameter 19.7 cm, mass 48.5 g) that was floating on pressurized air in a semi-spherical socket (Dombeck, Khabbaz, Collman, Adelman, & Tank, 2007), adapted from insect studies (Dahmen, 1980; Mason, Oshinsky, & Hoy, 2001; Stevenson, 2005). We used two optical computer mice to register the yaw and pitch of the ball (°/s) with a sampling rate of 60 Hz. Yaw is a proxy for the OLR because it is the axis of rotation of the visual stimulus. For each trial, we defined the mean OLR measured during the 500-ms period before motion onset as the baseline and subtracted it from the OLR-over-time trace. Because OLR could only be effectively measured as a deviation from forward locomotion, we excluded those trials in which the mice were sitting still by requiring a mean forward speed of at least 1 cm/s over the course of the trial. In further analysis, we required a minimum of 100 trials per condition per mouse. To smooth the OLR traces, we applied cubic splines using the csaps function of MATLAB.

Results

We measured the reflexive OLR to phi and reverse-phi single-step dot lifetime stimuli in nine mice. Figure 2a shows the mean and *SEM* of 129 OLRs in response to phi motion to the left (blue line) and 122 OLRs in response to phi motion to the right (red line) of one example mouse. The temporal

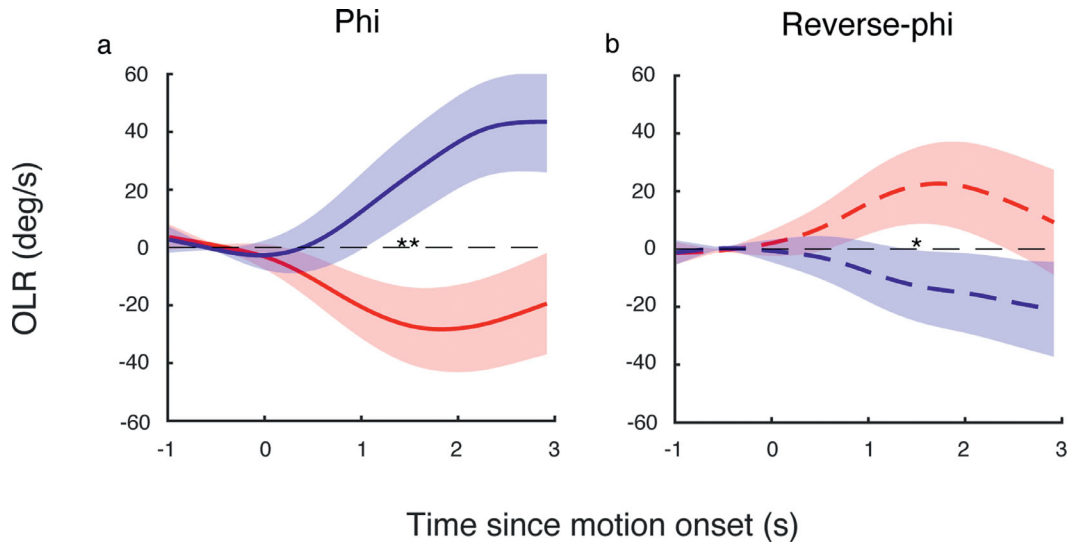

Figure 2. Comparison of OLR to phi and reverse-phi stimuli. (a) The mean opto-locomotor reflex over time for one mouse showing a typical OLR to rightward (red solid line) or leftward (blue solid line) phi stimuli. (b) Mean OLR for the same mouse to rightward (red dashed line) or leftward (blue dashed line) reverse-phi stimuli. The temporal interval in this example was 67 ms. Shaded bounds represent the *SEM*, asterisks indicate significant differences among OLRs (one-sided, two-sample *t*-test; $^{*}p < 0.05$, $^{**}p < 0.01$).

interval here was 67 ms. In our experiment, a positive stimulus speed corresponds to leftward displacement; therefore, Figure 2a shows that the mouse responded by attempting to turn in the same direction as the dots, as reported previously for unlimited lifetime stimuli (Kirkels et al., 2018). To test for differences between the blue and red OLRs, we averaged each trace over the interval from 1 to 2 seconds after stimulus onset and performed a one-sided, two-sample *t*-test where ($t(249) = –2.55$; $p = 0.006$). For reverse-phi stimuli the mouse responded with OLRs opposite to the direction of the moving patterns, as shown in Figure 2b ($t(254) = 1.87$; $p = 0.031$). This reversal is consistent with the human percept of reverse-phi stimuli and indicates that this mouse also experiences this motion illusion.

Figure 3 shows the variation within the population of all mice ($N = 9$) we recorded. We pooled the OLRs to leftward and rightward stimuli (red and blue curves in Figure 2) by taking the difference between them and dividing by two. We found that two animals from our pool, mouse 5 and mouse 7, did not respond in agreement with the behavior of the other animals. The opposite behavior of those two mice seemed consistent over frame durations; however, it should be noted that the OLRs of these two animals, together with those of mouse 4, are based on a duration condition of fewer than 100 trials per frame for both reverse-phi and phi stimuli, unlike the other animals.

We further explored the effect of temporal delay on the OLR by varying the frame duration from 17 to 117 ms in steps of 17 ms while maintaining the speed of displacement at 36°/s. Figure 4a shows the average response of six mice over time, excluding the three mice from the population that were left with fewer than 100 trials per frame duration condition for both reverse-phi (dashed lines) and phi stimuli (solid lines). We found significant divergence in the interval from 1 to 2 seconds after motion onset for the conditions with a delay of 17 ms ($t(5) = 7.76$; $p < 0.001$), 33 ms ($t(5) = 5.99$; $p < 0.001$), or 83 ms ($t(5) = 2.43$; $p < 0.05$) (Figure 4a). In Figure 4b, the pooled OLR is summarized as the mean between 1 and 2 seconds after motion onset. A frame duration of 33 ms resulted in the largest difference between responses to the phi and reverse-phi stimuli.

Discussion

Here we measured OLRs using our previously described head-fixed paradigm (Kirkels et al., 2018) to investigate whether mice perceive reverse-phi stimuli. Mice respond to changes in direction for phi stimuli and reverse-phi stimuli in opposite ways. Displacement of dot patterns in phi stimuli caused mice to reflexively compensate and adjust their running direction to the direction of the moving pattern. For the reverse-phi stimulus, however, mice responded by turning in the opposite direction to the dot displacement. This behavior is consistent with how human observers perceive phi and reverse-phi stimuli and is in accordance with psychophysical and neurophysiological findings

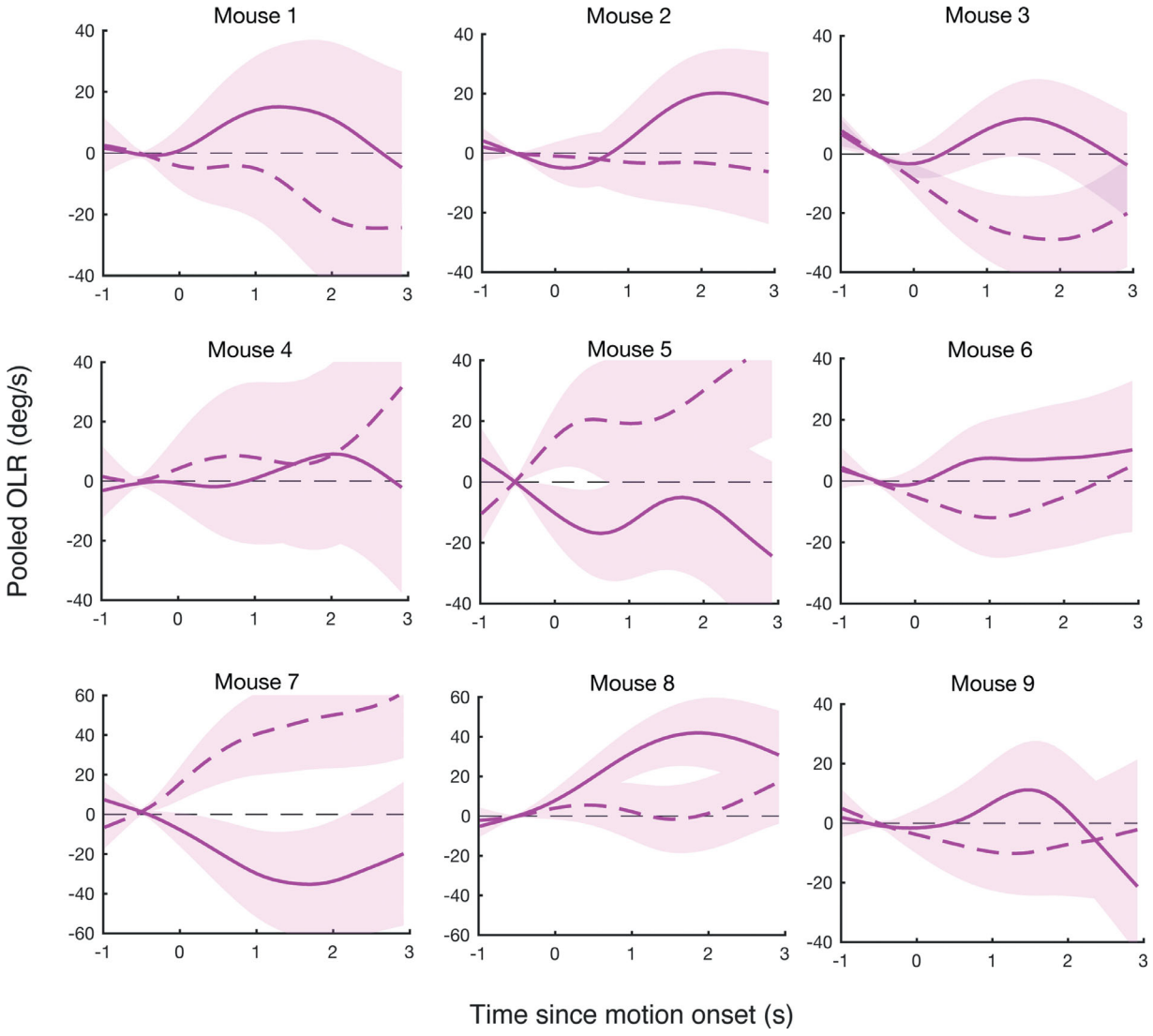

Figure 3. Pooled mean OLRs per animal to phi stimuli (solid line) and reverse-phi stimuli (dashed line) for frame duration of 33 ms. Shaded bounds represent the *SEM*.

from previous studies on reverse phi in other animals and humans (Bours et al., 2009; Clark et al., 2011; Emerson et al., 1987; Hassenstein & Reichardt, 1956; Ibbotson & Clifford, 2001; Krekelberg & Albright, 2005; Livingstone & Conway, 2003; Orger et al., 2000; Tuthill et al., 2011).

Our results show that the responses of mice are variable. First of all, the magnitude of the OLRs to phi and reverse-phi stimuli is considerably smaller than that for the OLRs we observed to unlimited lifetime motion stimuli we used in previous work (Kirkels et al., 2018). In the present study, the mean OLR peaks at about 15°/s with our most optimal parameter settings for perception of motion reversal, whereas our previous work reported a peak amplitude of about 30°/s. Although most parameters such as speed, contrast, and dot size were identical in these studies, an important difference was the use of single-step as opposed to unlimited lifetime for the dots, which is necessary for clean reverse-phi stimuli (Bours, Kroes, & Lankheet, 2007). Shortened dot lifetime has a negative effect on the signal-to-noise ratio of OLRs because more noise is present in the stimulus, which results in less motion energy in one direction (Hadad, Schwartz, Maurer, & Lewis, 2015). Two of the mice in our population showed other behavior with oppositely directed OLRs (Figure 3), which might be a result of this stimulus noise or because the number of successfully completed trials was less than for the other mice. It is also possible that the signal-to-noise ratio is different in these mice, as not all C57BL/6J mice have a fully functioning visual system. However, it is also possible that these two mice really have oppositely directed OLRs, and the underlying reason for this opposite behavior is unclear.

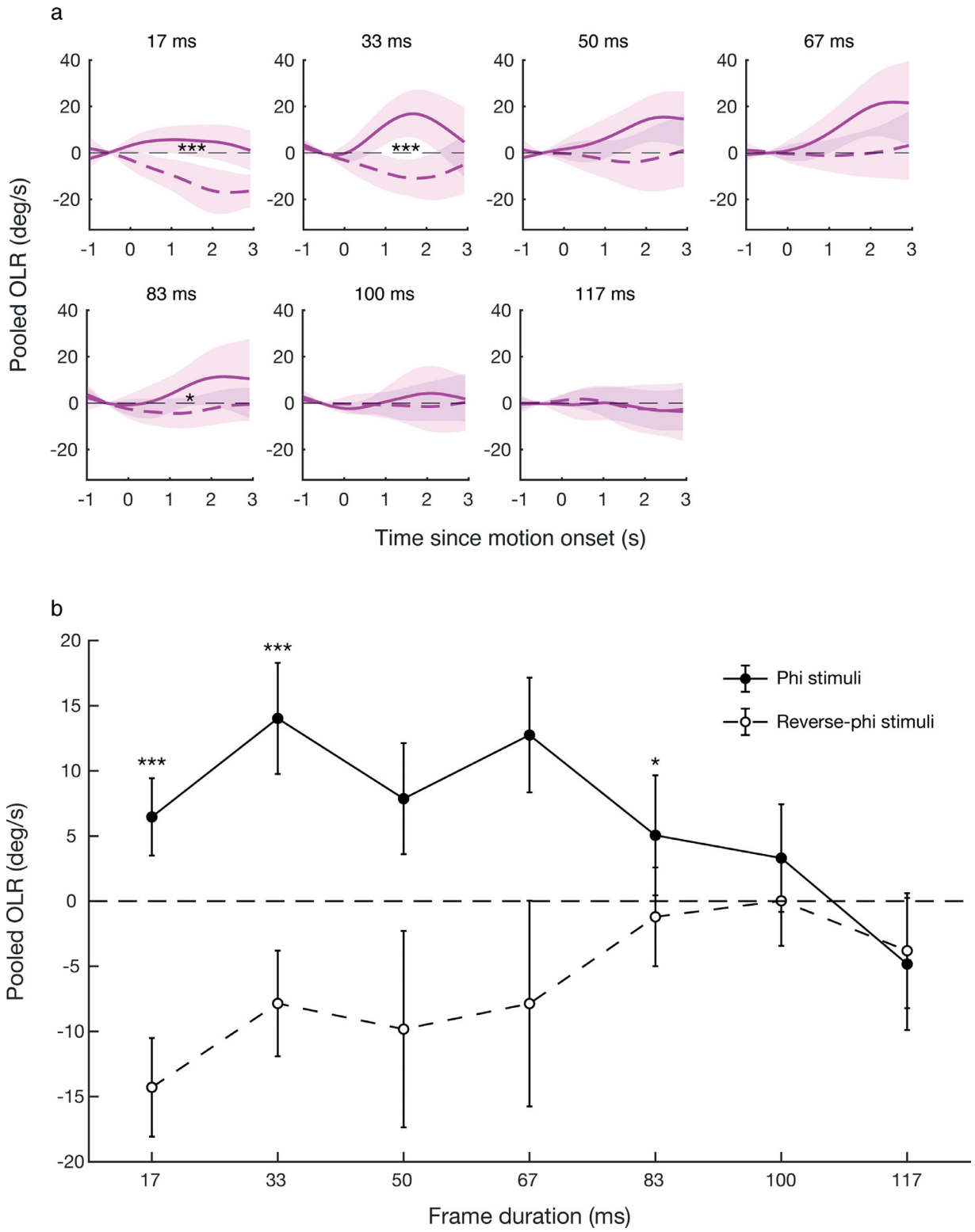

Figure 4. Effect of phi and reverse-phi stimuli on mice OLRs for different delays. (a) The mean opto-locomotor reflex over time of all animals ($n = 6$) to phi stimuli (solid line) and reverse-phi stimuli (dashed line) for seven different frame durations, pooled for leftward and rightward stimulus motion. Shaded bounds represent the *SEM*. (b) Mean OLR was summarized with a single number by taking the mean between 1 and 2 seconds after motion onset. Plotted for every frame duration is the pooled OLR to leftward and rightward motion for phi (solid line) and reverse-phi (dashed line) stimuli for all animals ($n = 6$). Error bars represent the *SEM*. Asterisks indicate significance levels of divergence ($^{*}p < 0.05$, $^{***}p < 0.001$; see main text for details).

We demonstrated a dependency of the OLR reversal effect on step interval. We found that the difference between the response to phi and reverse-phi stimuli is largest at a temporal interval of 33 ms. This is on the same order of magnitude as the slower delay filters mentioned in earlier studies in flies (Brinkworth & O'Carroll, 2009; Eichner, Joesch, Schnell, Reiff, & Borst, 2011; Shoemaker, O'Carroll, & Straw, 2005). A more recent fly study, however, showed maximal responses around a delay of 17 ms in both behavioral and neural measurements (Salazar-Gatzimas et al., 2016). It is important to note that results of these experiments might be specific for the chosen stimulus conditions. It has been shown in human psychophysical studies that perception of reverse-phi motion depends on many factors, such as stimulus eccentricity, spatial proximity, contrast, and spatial and temporal frequency (e.g., Anstis & Rogers, 1975; Benton, Johnston, & Mcowan, 1997; Bours et al., 2009; Chubb & Sperling, 1989; Edwards & Nishida, 2004; Oluk, Pavan, & Kafaligonul, 2016; Wehrhahn, 2006). Therefore, changes in our parameters such as dot size, step size, and stimulus speed could very well affect our finding.

Although the mean pooled OLR to reverse-phi was largest at a delay of 17 ms, the OLR to phi stimuli was almost entirely abolished at this delay. Why would the difference between phi and reverse-phi OLRs be so different at this step time? It should be noted that, to keep the dot speed always at 36°/s, the displacement from the first instance of the dot to the second was only 0.6°, or 1/5 of the dot diameter. Our data suggest that this was too small for the mouse to detect in the phi condition. In the reverse-phi condition, however, because the first and second instances are of opposite contrast polarity and displayed only briefly and in rapid succession, the overlapping parts in effect cancel each other and blend into the mid-gray background. We speculate that the strong response to the reverse-phi stimulus in this condition is driven by the black and white slivers visible at either side of this canceled-out region.

Keywords: reverse-phi, phi motion, opto-locomotor reflex, mice, illusion

Acknowledgments

This work was funded by NWO/MaGW 404-10-405.

Commercial relationships: none.
Corresponding author: Laurens A. M. H. Kirkels.
Email: laurenskirkels@gmail.com.
Address: Department of Biophysics, Donders Institute, Radboud University, Nijmegen, The Netherlands.

References

Adelson, E. H., & Bergen, J. R. (1985). Spatiotemporal energy models for the perception of motion. *Journal of the Optical Society of America A*, *2*(2), 284–299.

Akemann, W., Mutoh, H., Perron, A., Rossier, J., & Knöpfel, T. (2010). Imaging brain electric signals with genetically targeted voltage-sensitive fluorescent proteins. *Nature Methods*, *7*(8), 643–649, https://doi.org/10.1038/nmeth.1479.

Anstis, S. M. (1970). Phi movement as a subtraction process. *Vision Research*, *10*(12), 1411–1430, https://doi.org/10.1016/0042-6989(70)90092-1.

Anstis, S. M., & Mather, G. (1985). Effects of luminance and contrast on direction of ambiguous apparent motion. *Perception*, *14*(2), 167–179, https://doi.org/10.1068/p140167.

Anstis, S. M., & Rogers, B. J. (1975). Illusory reversal of visual depth and movement during changes of contrast. *Vision Research*, *15*, 957–961, https://doi.org/10.1016/0042-6989(75)90236-9.

Antic, S. D., Empson, R. M., & Knöpfel, T. (2016). Voltage imaging to understand connections and functions of neuronal circuits. *Journal of Neurophysiology*, *116*(1), 135–152, https://doi.org/10.1152/jn.00226.2016.

Benton, C. P., Johnston, A., & McOwan, P. W. (1997). Perception of motion direction in luminance- and contrast-defined reversed-phi motion sequences. *Vision Research*, *37*(17), 2381–2399, https://doi.org/10.1016/S0042-6989(97)00040-0.

Bours, R. J. E., Kroes, M. C. W., & Lankheet, M. J. (2009). Sensitivity for reverse-phi motion. *Vision Research*, *49*(1), 1–9, https://doi.org/10.1016/j.visres.2008.09.014.

Bours, R. J. E., Kroes, M. C. W., & Lankheet, M. J. M. (2007). The parallel between reverse-phi and motion aftereffects. *Journal of Vision*, *7*(11), 1–10, https://doi.org/10.1167/7.11.8.Introduction.

Bours, R. J. E., Stuur, S., & Lankheet, M. J. M. (2007). Tuning for temporal interval in human apparent motion detection. *Journal of Vision*, *7*(1), 2, https://doi.org/10.1167/7.1.2.

Brinkworth, R. S. A., & O'Carroll, D. C. (2009). Robust models for optic flow coding in natural scenes inspired by insect biology. *PLoS Computational Biology*, *5*(11), e1000555, https://doi.org/10.1371/journal.pcbi.1000555.

Calkins, D. J., Tsukamoto, Y., Sterling, P., & Euler, T. (1998). Microcircuitry and mosaic of a blue-yellow ganglion cell in the primate retina. *Journal of Neuroscience*, *18*(9), 3373–3385, https://doi.org/10.1523/jneurosci.0616-11.2011.

Chen, T.-W., Wardill, T. J., Sun, Y., Pulver, S. R., Renninger, S. L., Baohan, A., . . . Kim, D. S. (2013). Ultrasensitive fluorescent proteins for imaging neuronal activity. *Nature*, *499*(7458), 295–300, https://doi.org/10.1038/nature12354.

Chubb, C., & Sperling, G. (1989). Two motion perception mechanisms revealed through distance-driven reversal of apparent motion. *Proceedings of the National Academy of Sciences U S A*, *86*(8), 2985–2989, https://doi.org/10.1073/pnas.86.8.2985.

Clark, D. A., Bursztyn, L., Horowitz, M. A., Schnitzer, M. J., & Clandinin, T. R. (2011). Defining the computational structure of the motion detector in *Drosophila*. *Neuron*, *70*(6), 1165–1177, https://doi.org/10.1016/j.neuron.2011.05.023.

Dahmen, H. J. (1980). A simple apparatus to investigate the orientation of walking insects. *Experientia*, *36*(6), 685–687, https://doi.org/10.1007/BF01970140.

Dombeck, D. A., Khabbaz, A. N., Collman, F., Adelman, T. L., & Tank, D. W. (2007). Imaging large-scale neural activity with cellular resolution in awake, mobile mice. *Neuron*, *56*(1), 43–57, https://doi.org/10.1016/j.neuron.2007.08.003.

Duijnhouwer, J., & Krekelberg, B. (2016). Evidence and counterevidence in motion perception. *Cerebral Cortex*, *26*(12), 4602–4612, https://doi.org/10.1093/cercor/bhv221.

Edwards, M., & Nishida, S. (2004). Contrast-reversing global-motion stimuli reveal local interactions between first- and second-order motion signals. *Vision Research*, *44*(16), 1941–1950, https://doi.org/10.1016/j.visres.2004.03.016.

Eichner, H., Joesch, M., Schnell, B., Reiff, D. F., & Borst, A. (2011). Internal structure of the fly elementary motion detector. *Neuron*, *70*(6), 1155–1164, https://doi.org/10.1016/j.neuron.2011.03.028.

Ekesten, B., & Gouras, P. (2005). Cone and rod inputs to murine retinal ganglion cells: Evidence of cone opsin specific channels. *Visual Neuroscience*, *22*(6), 893–903, https://doi.org/10.1017/S0952523805226172.

Emerson, R. C., Citron, M. C., Vaughn, W. J., & Klein, S. A. (1987). Nonlinear directionally selective subunits in complex cells of cat striate cortex. *Journal of Neurophysiology*, *58*(1), 33–65.

Fenno, L., Yizhar, O., & Deisseroth, K. (2011). The development and application of optogenetics. *Annual Review of Neuroscience*, *34*(1), 389–412, https://doi.org/10.1146/annurev-neuro-061010-113817.

Ghosh, K. K., Bujan, S., Haverkamp, S., Feigenspan, A., & Wässle, H. (2004). Types of bipolar cells in the mouse retina. *Journal of Comparative Neurology*, *469*(1), 70–82, https://doi.org/10.1002/cne.10985.

Grubb, M. S., & Thompson, I. D. (2004). Biochemical and anatomical subdivision of the dorsal lateral geniculate nucleus in normal mice and in mice lacking the $\beta 2$ subunit of the nicotinic acetylcholine receptor. *Vision Research*, *44*(28), 3365–3376, https://doi.org/10.1016/j.visres.2004.09.003.

Hadad, B., Schwartz, S., Maurer, D., & Lewis, T. L. (2015). Motion perception: a review of developmental changes and the role of early visual experience. *Frontiers in Integrative Neuroscience*, *9*, 49, https://doi.org/10.3389/fnint.2015.00049.

Han, X., Qian, X., Bernstein, J. G., Zhou, H.-H., Franzesi, G. T., Stern, P., . . . Boyden, E. S. (2009). Millisecond-timescale optical control of neural dynamics in the nonhuman primate brain. *Neuron*, *62*(2), 191–198, https://doi.org/10.1016/j.neuron.2009.03.011.

Harvey, C. D., Collman, F., Dombeck, D. A., & Tank, D. W. (2009). Intracellular dynamics of hippocampal place cells during virtual navigation. *Nature*, *461*(7266), 941–946, https://doi.org/10.1038/nature08499.

Hassenstein, B., & Reichardt, W. (1956). Systemtheoretische Analyse der Zeit-, Reihenfolgen- und Vorzeichenauswertung bei der Bewegungsperzeption des Rüsselkäfers Chlorophanus. *Zeitschrift Für Naturforschung B*, *11*(9–10), 513–524.

Hölscher, C., Schnee, A., Dahmen, H., Setia, L., & Mallot, H. A. (2005). Rats are able to navigate in virtual environments. *Journal of Experimental Biology*, *208*(Pt. 3), 561–569.

Huberman, A. D., & Niell, C. M. (2011). What can mice tell us about how vision works? *Trends in Neurosciences*, *34*(9), 464–473, https://doi.org/10.1016/j.tins.2011.07.002.

Huberman, A. D., Wei, W., Elstrott, J., Stafford, B. K., Feller, M. B., & Barres, B. A. (2009). Genetic identification of an on-off direction-selective retinal ganglion cell subtype reveals a layer-specific subcortical map of posterior motion, *62*(3), 327–334, https://doi.org/10.1016/j.neuron.2009.04.014.Genetic.

Ibbotson, M. R., & Clifford, C. W. (2001). Interactions between ON and OFF signals in directional motion detectors feeding the not of the wallaby. *Journal of Neurophysiology*, *86*(2), 997–1005.

Kirkels, L. A. M. H., Zhang, W., Havenith, M. N., Tiesinga, P., Glennon, J., Wezel, R. J. A. Van, . . . Duijnhouwer, J. (2018). The opto-locomotor reflex as a tool to measure sensitivity to moving random dot patterns in mice. *Scientific Reports*, *8*(1), 7710, https://doi.org/10.1038/s41598-018-25844-4.

Knöpfel, T. (2012). Genetically encoded optical indicators for the analysis of neuronal circuits.

Nature Reviews Neuroscience, *13*(10), 687–700, https://doi.org/10.1038/nrn3293.

Krekelberg, B., & Albright, T. D. (2005). Motion mechanisms in macaque MT. *Journal of Neurophysiology*, *93*(5), 2908–2921, https://doi.org/10.1152/jn.00473.2004.

Leonhardt, A., Meier, M., Serbe, E., Eichner, H., & Borst, A. (2017). Neural mechanisms underlying sensitivity to reverse-phi motion in the fly. *PLoS ONE*, *12*(12), 1–25, https://doi.org/10.1371/journal.pone.0189019.

Livingstone, M. S., & Conway, B. R. (2003). Substructure of direction-selective receptive fields in macaque V1. *Journal of Neurophysiology*, *89*(5), 2743–2759, https://doi.org/10.1152/jn.00822.2002.

Mason, A. C., Oshinsky, M. L., & Hoy, R. R. (2001). Hyperacute directional hearing in a microscale auditory system. *Nature*, *410*(6829), 686–690, https://doi.org/10.1038/35070564.

Mataruga, A., Kremmer, E., & Müller, F. (2007). Type 3a and type 3b OFF cone bipolar cells provide for the alternative rod pathway in the mouse retina. *Journal of Comparative Neurology*, *502*(6), 1123–1137, https://doi.org/10.1002/cne.21367.

Miyawaki, A., Llopis, J., Heim, R., McCaffery, J. M., Adams, J. A., Ikura, M., … Tsien, R. Y. (1997). Fluorescent indicators for Ca2+ based on green fluorescent proteins and calmodulin. *Nature*, *388*(6645), 882–887, https://doi.org/10.1038/42264.

Mo, C.-H., & Koch, C. (2003). Modeling reverse-phi motion-selective neurons in cortex: Double synaptic-veto mechanism. *Neural Computation*, *15*(4), 735–759, https://doi.org/10.1162/08997660360581886.

Morgan, M. J., & Ward, R. (1980). Conditions for motion flow in dynamic visual noise. *Vision Research*, *20*(5), 431–435.

Niell, C. M., & Stryker, M. P. (2008). Highly selective receptive fields in mouse visual cortex. *Journal of Neuroscience*, *28*(30), 7520–7536.

Oluk, C., Pavan, A., & Kafaligonul, H. (2016). Rapid motion adaptation reveals the temporal dynamics of spatiotemporal correlation between on and off pathways. *Scientific Reports*, *6*, 34073, https://doi.org/10.1038/srep34073.

Orger, M. B., Smear, M. C., Anstis, S. M., & Baier, H. (2000). Perception of Fourier and non-Fourier motion by larval zebrafish. *Nature Neuroscience*, *3*(11), 1128–1133, https://doi.org/10.1038/80649.

Packer, A. M., Roska, B., & Häusser, M. (2013). Targeting neurons and photons for optogenetics. *Nature Neuroscience*, *16*(7), 805–815, https://doi.org/10.1038/nn.3427.

Priebe, N. J., & McGee, A. W. (2014). Mouse vision as a gateway for understanding how experience shapes neural circuits. *Frontiers in Neural Circuits*, *8*, 123, https://doi.org/10.3389/fncir.2014.00123.

Prusky, G. T., & Douglas, R. M. (2003). Developmental plasticity of mouse visual acuity. *European Journal of Neuroscience, 17*(1), 167–173, https://doi.org/10.1046/j.1460-9568.2003.02420.x.

Puller, C., & Haverkamp, S. (2011). Bipolar cell pathways for color vision in non-primate dichromats. *Visual Neuroscience*, *28*(1), 51–60, https://doi.org/10.1017/S0952523810000271.

Salazar-Gatzimas, E., Agrochao, M., Fitzgerald, J. E., & Clark, D. A. (2018). The neuronal basis of an illusory motion percept is explained by decorrelation of parallel motion pathways. *Current Biology*, *28*(23), 3748–3762.e8, https://doi.org/https://doi.org/10.1016/j.cub.2018.10.007.

Salazar-Gatzimas, E., Chen, J., Creamer, M. S., Mano, O., Mandel, H. B., Matulis, C. A., … Clark, D. A. (2016). Direct measurement of correlation responses in Drosophila elementary motion detectors reveals fast timescale tuning. *Neuron*, *92*(1), 227–239, https://doi.org/10.1016/j.neuron.2016.09.017.

Schiller, P. H. (1992). The ON and OFF channels of the visual system. *Trends in Neurosciences*, *15*(3), 86–92, https://doi.org/10.1016/0166-2236(92)90017-3.

Schmidt-Hieber, C., & Häusser, M. (2013). Cellular mechanisms of spatial navigation in the medial entorhinal cortex. *Nature Publishing Group*, *16*(3), 325–331, https://doi.org/10.1038/nn.3340.

Shoemaker, P. A., O'Carroll, D. C., & Straw, A. D. (2005). Velocity constancy and models for wide-field visual motion detection in insects. *Biological Cybernetics*, *93*(4), 275–287, https://doi.org/10.1007/s00422-005-0007-y.

Sternson, S. M., & Roth, B. L. (2014). Chemogenetic tools to interrogate brain functions. *Annual Review of Neuroscience*, *37*(1), 387–407, https://doi.org/10.1146/annurev-neuro-071013-014048.

Stevenson, P. A. (2005). Octopamine and experience-dependent modulation of aggression in crickets. *Journal of Neuroscience*, *25*(6), 1431–1441, https://doi.org/10.1523/JNEUROSCI.4258-04.2005.

Tian, L., Hires, S. A., Mao, T., Huber, D., Chiappe, M. E., Chalasani, S. H., … Looger, L. L. (2009). Imaging neural activity in worms, flies and mice with improved GCaMP calcium indicators. *Nature Methods*, *6*(12), 875–881, https://doi.org/10.1038/nmeth.1398.

Tuthill, J. C., Chiappe, M. E., & Reiser, M. B. (2011). Neural correlates of illusory motion perception

in Drosophila. *Proceedings of the National Academy of Sciences U S A*, *108*(23), 9685–9690, https://doi.org/10.1073/pnas.1100062108.

van Santen, J. P., & Sperling, G. (1985). Elaborated Reichardt detectors. *Journal of the Optical Society of America A*, *2*(2), 300–321.

Volland, S., Esteve-Rudd, J., Hoo, J., Yee, C., & Williams, D. S. (2015). A comparison of some organizational characteristics of the mouse central retina and the human macula. *PLoS One*, *10*(4), 1–13, https://doi.org/10.1371/journal.pone.0125631.

Wang, Q., Gao, E., & Burkhalter, A. (2011). Gateways of ventral and dorsal streams in mouse visual cortex. *Journal of Neuroscience*, *31*(5), 1905–1918, https://doi.org/10.1523/JNEUROSCI.3488-10.2011.

Wehrhahn, C. (2006). Reversed phi revisited. *Journal of Vision*, *6*(10), 1018–1025, https://doi.org/10.1167/6.10.2.

Westheimer, G. (2007). The ON–OFF dichotomy in visual processing: From receptors to perception. *Progress in Retinal and Eye Research*, *26*(6), 636–648, https://doi.org/10.1016/j.preteyeres.2007.07.003.

Wong, A. A., & Brown, R. E. (2006). Visual detection, pattern discrimination and visual acuity in 14 strains of mice. *Genes, Brain and Behavior*, *5*(5), 389–403, https://doi.org/10.1111/j.1601-183X.2005.00173.x.

Wulff, P., & Arenkiel, B. R. (2012). Chemical genetics: receptor-ligand pairs for rapid manipulation of neuronal activity. *Current Opinion in Neurobiology*, *22*(1), 54–60, https://doi.org/10.1016/j.conb.2011.10.008.

Zhang, F., Wang, L.-P., Brauner, M., Liewald, J. F., Kay, K., Watzke, N., … Deisseroth, K. (2007). Multimodal fast optical interrogation of neural circuitry. *Nature*, *446*(7136), 633–639, https://doi.org/10.1038/nature05744.